Anal Bioanal Chem (2008) 391:1837–1844
DOI 10.1007/s00216-008-1904-4

ORIGINAL PAPER

A new optical platform for biosensing based on fluorescence anisotropy

F. Baldini · A. Carloni · A. Giannetti · G. Porro · C. Trono

Received: 30 November 2007 / Revised: 17 January 2008 / Accepted: 21 January 2008 / Published online: 15 February 2008

Abstract A novel fluorescence-based optical platform for the interrogation of an optical biochip was designed and developed. The optical biochip was made of poly(methyl methacrylate) (PMMA) formed by two pieces of PMMA appropriately shaped in order to obtain four microchannels that are 500-μm wide and 400-μm high. The lower part includes the microchannels and the inlet and outlet for the fluidics, while the sensing biolayer was immobilized on the upper part. The optical signal comprised the fluorescence emitted by the biolayer, which was anisotropically coupled to the PMMA cover and suitably guided by the PMMA chip. The potentiality of the optical chip as a biosensor was investigated by means of a direct IgG/anti-IgG interaction carried out inside the flow channels. The mouse-IgG was covalently immobilized on the internal wall of the PMMA cover, and the Cy5-labelled anti-mouse IgG was used for the specific interaction. Several chemical treatments of the PMMA surface were investigated, poly(L-lactic acid), Eudragit L100 and NaOH, in order to obtain the most effective distribution of carboxylic groups useful for the covalent immobilisation of the mouse-IgG. The treatment with Eudragit L100 was found to be the most successful. Limits of detection and quantification of 0.05 μg mL^{-1} and 0.2 μg mL^{-1}, respectively, were obtained with the configuration described.

F. Baldini (✉) · A. Carloni · A. Giannetti · C. Trono
Institute of Applied Physics, CNR,
Via Madonna del Piano 10,
50019 Sesto Fiorentino (FI), Italy
e-mail: f.baldini@ifac.cnr.it

G. Porro
Datamed S.r.L.,
Via Papa Giovanni XXIII 45,
20090 Rodano (MI), Italy

Keywords Optical biosensor · Optical chip · PMMA · Fluorescence anisotropy · IgG

Introduction

Rapid, simple and low-cost medical devices for multiple parameter screening are essential for early diagnosis and improved treatments of diseases and infectious illness. One solution to this significant demand requires the advent of new and more reliable biosensors integrated within the same biochip. Biosensors are diagnostic devices that exploit the powerful molecular recognition capability of bioreceptors such as antibodies, enzymes, DNA, aptamers and scaffolds. A biochip can be considered an array of biosensors that are individually monitored and are generally used contemporaneously for the determination of multiple analytes [1, 2]. Thanks to miniaturization, low cost and potential for large-scale automation, biochips can perform analyses more efficiently than currently available laboratory equipment. In the design and development of compact and inexpensive biochips, optics can play a relevant role owing to (1) the ease of attaining an optical transduction for the detection of bioanalytes [3], (2) versatility of optical and optoelectronic components (3) the capability of CCD detectors to analyse thousands of sensing spots. A major distinction between optical biochips can be made: label-free systems [4–6] are those in which the interaction analyte/sensitive layer gives rise to a modification of the optical signal due to a change in the refractive index of the layer deposited on the substrate, and label-based systems [7–11] are those in which the optical signal that depends on the analyte investigated comes from a label with suitable optical properties (mainly fluorescent or chemiluminescent labels). There are both advantages and disadvantages present in

these two methods. The main advantage of a direct detection method is its capability to make analyses without the application of labels [12]. In fact, label-based biosensors require either multistep detection protocols or delicately balanced affinities of interacting biomolecules for displacement assays, which can cause sensor cross-sensitivity to nontarget analytes. However, for complex sample monitoring, the label-free methods continue to be susceptible to problems such as low sensitivity and increased background due to nonspecific binding. Therefore, in clinical applications in which the sample matrix can be very complex (e.g. whole blood or serum) the use of a label-based system may be preferable [13]. Moreover, any changes in the sensing surface, e.g. due to nonspecific adsorption or fouling, give rise to a perturbation of the refractive index which is the measured parameter in the label-free system. In the label-based system this perturbation takes place only if these changes modify the interaction between the immobilised bioreceptor and the labelled marker.

In general, the optical biochip is characterised by a miniaturised arrangement of immobilised reagents in micrometric spots on glass substrates, such as microscope slides, and fluorescence scanners are used for the chip readout [14]. In the case of proteomics or nucleic acid applications, a large number of spots, of the order of thousands, are necessary for gene expression profiling. Therefore, one recent market trend has been the development of fluorescence optical readers that are capable of reading hundreds or thousands of spots. Clearly, all these instruments are part of laboratory instrumentation; they are usually cumbersome, and are extremely expensive. On the other hand, in many clinical applications the measurement of a limited number of parameters (5–15) is sufficient to help physicians in the diagnosis of pathologies or in the choice of the appropriate therapy. Another important aspect which has not been properly considered in the design of optical readers is that these devices collect fluorescence signals from the top or the bottom of the biochip without considering the anisotropy of the fluorescence. The presence of a fluorophore in the proximity of a solid/liquid interface [15, 16] implies the existence of preferential directions in the emission fluorescence, and disregarding this behaviour can give rise to detection processes that are very low in efficiency.

In a previous paper, an optical platform for the interrogation of a multichannel array for chemical and biochemical parameters was described [17]. The optical platform consists of a plastic chip formed by two pieces of poly(methyl methacrylate) (PMMA) that are suitably shaped in order to obtain several flow channels. Light from a laser or LED is used to excite the fluorescent-sensing layer immobilized on the internal wall of the channel. The emitted light travels along the thickness of the PMMA cover and is detected with an optical fibre connected to a photodetector. Preliminary tests were carried out by immobilising a pH indicator, fluorescein, in the PMMA channel and then evaluating the optical efficiency of the system.

The present paper is concerned with the optimisation of the optical platform in terms of excitation and detection efficiency, with the implementation of an effective immobilisation procedure that is used to immobilise a bioreceptor on the PMMA substrate and with the characterisation of the optical system with an IgG/anti-IgG immunoassay. Here, a single channel is characterised, using a single source and a single detector, with the purpose of demonstrating the efficiency of the system.

Materials and methods

Materials

All the following chemicals were purchased from Sigma (Sigma-Aldrich S.r.l., Milan, Italy): sodium chloride (NaCl), disodium hydrogen phosphate (Na_2HPO_4), potassium chloride (KCl), ethanol (EtOH), sodium hydroxide (NaOH), chloroform ($CHCl_3$), morpholinesulfonic acid monohydrate (MES), dimethylsulfoxide (DMSO), 2-amino-2-(hydroxymethyl)-1,3-propanediol, hydrochloride (tris-HCl).

Poly(methyl methacrylate) (PMMA) planar slides (1.5-mm and 3-mm thickness) were purchased from RS Components, Milan, Italy. Poly(L-lactic acid) (PLLA) was purchased from DURECT Corporation, Cupertino, California. The methacrylic acid/methacrylate copolymer (Eudragit L100) was purchased from Degussa, Röhm Pharma Polymers, Evonik Degussa GmbH, Düsseldorf, Germany.

The mouse-IgG and Cy5-labelled anti-mouse-IgG were purchased from Zymed Laboratories, Invitrogen Immunodetection, Milan, Italy. 1-Ethyl-3-[3-dimethylaminopropyl] carbodiimide hydrochloride (EDC) and *N*-hydroxysuccinimide (NHS) were purchased from Pierce, Rockford, Illinois, USA.

The optical source used was a laser diode (LD) emitting at 635 nm with 3-mW output power (Hitachi HL6314MG). A band-pass (BP) filter, at 635 nm (Thorlabs FL635-10), with 10-nm full width at half maximum, and a high-pass (HP) filter, cut-on at 650 nm (Thorlabs FEL0650) were purchased from Thorlabs GMBH, Dachau, Germany. Graded index (GRIN) lenses, 1/4 pitch, 1.8-mm diameter were purchased from SELFOC Microlens, NSG Europe, Temse, Belgium; optical fibres, 200 μm in core diameter, came from Polymicro Technologies, Phoenix, Arizona, USA. Two optical spectrum analyzers, Ocean Optics S2000 (Dunedin, Florida, USA) and Hamamatsu TG-SWNIR CCD (C9405CA) (Hamamatsu Photonics Italia S. R.L., Arese (MI), Italy), were used as detector systems.

A peristaltic pump (Minipulse 3-Gilson, Gilson Inc., Middleton, Wisconsin, USA) and poly(vinyl chloride)

(PVC) tubing (i.d. 0.76 mm - Gilson) were used for the fluidic system.

O-ring gaskets (inner diameter 11.60 mm, cross section 0.40 mm), used to seal the microchannels, were purchased from ISO SWISS Watch parts, Boecourt, Switzerland.

Surface modification

The PMMA surface was treated according to the following protocols in order to covalently immobilise mouse-IgG via interaction of their amino groups with carboxylic groups present on the solid support. The carboxylic groups were obtained by means of:

1. Treatment with 2 M NaOH in pure water and in a mixture of water/DMSO (1:1) for 1 h, and then washing with deionised water;
2. Deposition of Eudragit L100 in 95% EtOH at different concentrations (0.001–100 mM) until evaporation of the solvent, and then washing with deionised water;
3. Deposition of PLLA in $CHCl_3$ at different concentrations (0.01–10 mM) until evaporation of the solvent; then, after washing with deionised water, treatment with 2 M NaOH and further washing with deionised water.

The carboxylic groups present on the surface were activated by means of EDC (2 mM) and NHS (5 mM) in MES buffer 0.1 M at pH 6.2. After 30 min, the channel was rinsed MES buffer and then PBS buffer (137 mM NaCl, 10 mM Na_2HPO_4, 2.7 mM KCl, pH 7.4).

The treatments described above were carried out on different PMMA substrates. The PMMA planar slides were modified to obtain two different configurations: small planar square and four-channel chip. In the first case, the 1.5-mm-thick planar slide was cut with a laser into small squares (1 cm × 1 cm) that were used to evaluate the different surface treatments. The second configuration, the PMMA chip, which was used to implement the IgG/anti-IgG immunoassay, was obtained from the 3-mm-thick planar slide by following an appropriate inhouse processing using mechanical tools. The chip consists of four channels, obtained by combining two pieces: the lower part, which includes the four microchannels and the inlet and outlet for the fluidics, and the upper part, on which the sensing layer is immobilized (Fig. 1). The dimensions of a single flow channel are 0.5-mm width, 0.4-mm height and 18-mm length.

Immunoassay protocols

An excess of mouse IgG in PBS (1.25 mg mL^{-1}) was dropped onto the small squares, left for 1 h for the immobilization procedure to take place, and then rinsed with PBS. The immobilisation was then followed by incubation for 1 h with a high concentration (1 mg mL^{-1}) of the Cy5-labelled anti-mouse-IgG and by successive rinsing with PBS in order to remove the excess labelled anti-mouse-IgG.

In the case of the PMMA chip, the IgG immobilisation and the assay were carried out under flow conditions. The PMMA chip was connected to the peristaltic pump by means of the PVC tubing. The flow rate used in all the experiments was 30 μL min^{-1}. Different concentrations of mouse-IgG (0.5–0.005 mg mL^{-1}) were immobilised on the channels (interaction time 30 min) and then rinsed with PBS. Moreover, different concentrations of labelled anti-mouse-IgG (1 ng mL^{-1}–100 μg mL^{-1}) were tested by following the developed protocol, with 15 min of incubation time for the immunoassay and 5 min for PBS washing.

Optical systems

Two different optical systems have been developed in order to characterise the small planar square and the four-channel array chip. The first one, which was developed for the interrogation

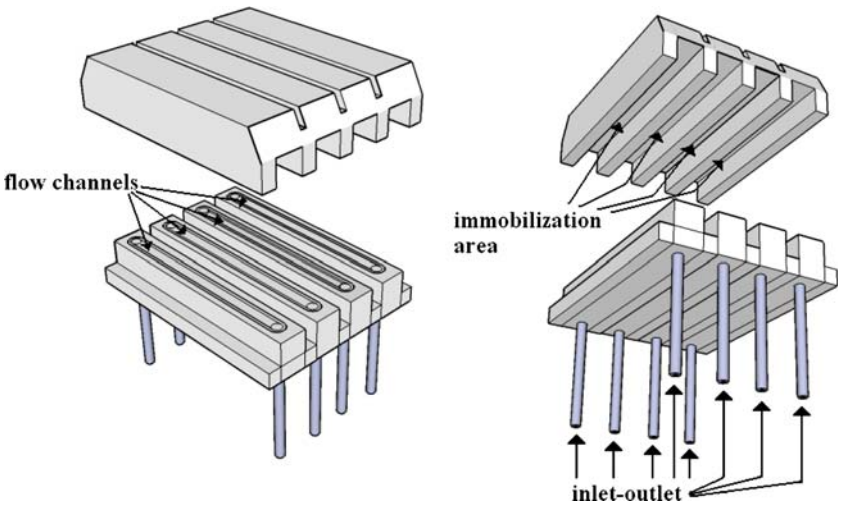

Fig. 1 Exploded view of the PMMA chip with the top and bottom parts separated. Two different views are drawn allowing the flow channels and the immobilisation area to be seen

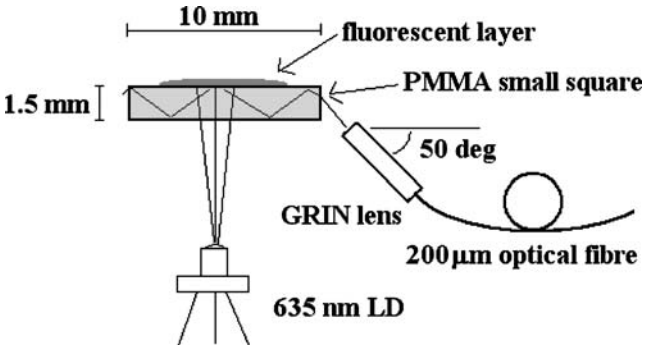

Fig. 2 Optical setup for the small planar squares

of the planar square, is illustrated in Fig. 2. The fluorescent layer was excited by means of the LD at 635 nm, depending on the fluorophore used (Cy5). The fluorescence, which is preferably emitted with an angle of 60° with respect to the direction normal to the interface inside the PMMA, was collected from one side of the chip by means of a GRIN lens coupled with an optical fibre. Considering the refraction at the PMMA/air interface on the lateral surface of the small planar square, the fluorescent light was efficiently collected at an angle of roughly 50° with respect to the normal to the interface. The signal was then analysed by means of the Ocean Optics S2000 spectrometer.

The optical setup for the multichannel array interrogation is illustrated in Fig. 3. The excitation source was the LD at 635 nm, filtered by means of the BP filter centred at 635 nm. A homemade plastic cylindrical piano-convex lens located on the cover of the chip (Fig. 3) leads to an improvement of the excitation efficiency. A fraction of the fluorescence emitted by the sensing layer immobilised on the bottom of the PMMA cover travels along the thickness of the PMMA up to its end-face where it was collected by means of a multimode optical fibre coupled with the GRIN lens. The end-face of the cover was polished at 60° to facilitate the alignment with the collecting fibre. The particular profile of the cover with the presence of air gaps, as shown in Fig. 3b, allows a physical separation of the fluorescent signal coming from the different channels, so that each channel is optically separated from the others. The fluorescence collected was filtered with the 650-nm HP filter and analysed with the Hamamatsu spectrometer.

Results and discussion

The small PMMA squares were used for a preliminary evaluation of the different surface treatments, which were performed to obtain carboxylic groups on the solid support that could be useful for the covalent immobilisation of the bioreceptor.

Treatments with PLLA, Eudragit L100 and NaOH were compared by immobilising excess mouse-IgG and making the sensing layers obtained react with a concentrated solution of Cy5-labelled anti-mouse-IgG, as described in the Materials and methods. The emitted fluorescence was then measured with the optical setup shown in Fig. 2 in which the 635-nm LD was used as source and was driven by a current of 30 mA, and the Ocean Optics spectrometer was adjusted to allow an integration time of 5,000 ms. The choice of the source at 635 nm, where the excitation efficiency of Cy5 is roughly 65%, follows the criterion of achieving a good separation between the excitation and emission wavelengths used.

Figure 4 shows the typical fluorescence spectra of the small PMMA squares treated with a PLLA concentration of 0.01–10 mM. The results are summarised in the histogram of Fig. 5, in which the columns were obtained by evaluating the integral of the fluorescence spectra between 650 and 750 nm. The error bar was the standard deviation on three measurements made on three different squares. As can be seen from the histogram, the concentration of carboxylic groups on the PMMA surface was a critical value: the measured fluorescence increased with a decrease in the PLLA concentration, i.e. with a decrease in the COOH concentrations on the PMMA surface.

The reason of this behaviour can be ascribed to a twofold effect:

– An overly large concentration of exposed functional groups led to an excessive and unordered immobilisa-

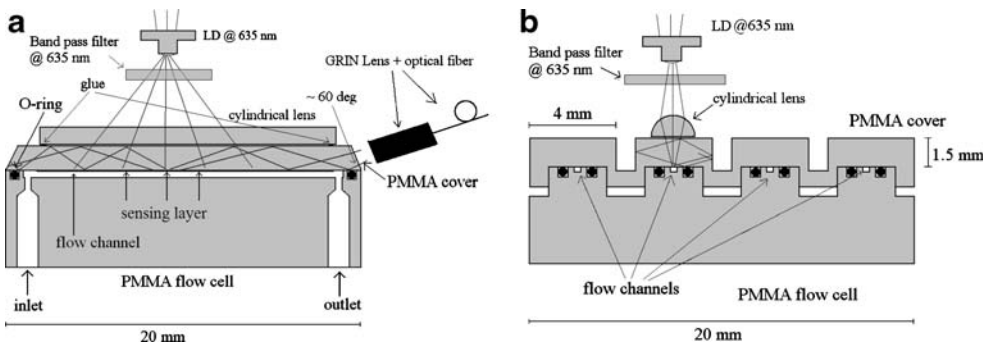

Fig. 3 Longitudinal section (**a**) and cross section (**b**) of the optical setup for the multichannel array interrogation

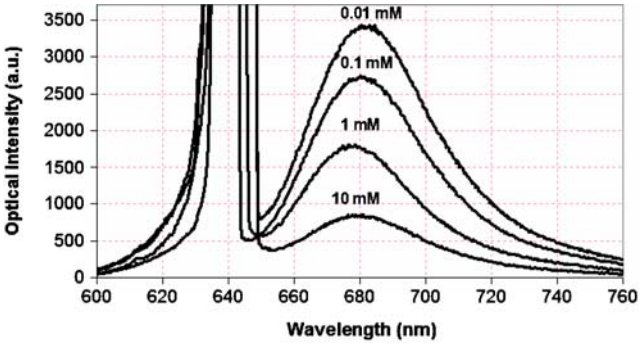

Fig. 4 Fluorescence emission spectra of the small PMMA squares treated with a PLLA concentration of 0.01–10 mM, measured with the optical setup shown in Fig. 2. The detected light at almost 635 nm is the contribution coming from the LD due to the scattering

tion of IgG molecules; the resulting steric hindrance and interaction between the IgG themselves caused a lower affinity toward the labelled anti-IgG;

– An excessive density of the fluorophore can give rise to inner filter effects with the reabsorption of the emitted fluorescence by the same fluorophore.

On the other hand, it is reasonable to expect a decrease of fluorescence if the COOH concentration decreased too much since this will also correspond to a decrease of the labelled anti-IgG which interacts with the immobilised IgG. This was observed in the case of the treatment of the PMMA surface with Eudragit L100. Figure 6 shows the histogram for six different concentrations of Eudragit L100. The trend was the same as that observed for PLLA: by decreasing the concentration of Eudragit, an increase of the detected fluorescence was observed. However, a further decrease beyond 0.01 mM caused a decrease in the detected signal, showing that the optimum concentration of Eudragit L100 on the PMMA surface was 0.01 mM.

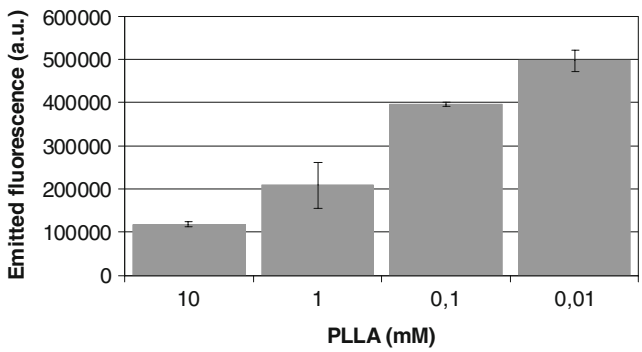

Fig. 5 Histogram of the emitted fluorescence of the small squares treated with PLLA at different concentrations (10–0.01 mM), evaluated by considering the area of the collected spectra shown in Fig. 4 between 650 and 750 nm. The *error bars* give the standard deviations on three measurements performed on three different squares

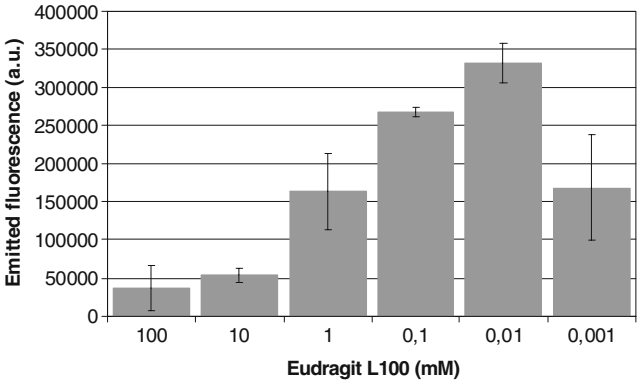

Fig. 6 Histogram of the emitted fluorescence of the small squares treated with Eudragit L100 at different concentrations (100–0.001 mM), evaluated by considering the area of the collected spectra between 650 and 750 nm. The *error bars* give the standard deviations on three measurements performed on three different squares

The results obtained with NaOH are summarised in Fig. 7. The treatment with NaOH in pure water was not very effective. Better results were obtained with NaOH dissolved in a 1:1 mixture of water and DMSO since this increases the wettability of the PMMA and causes a better interaction between the solution with surface.

The nonspecific binding of labelled anti-IgG on the treated PMMA was tested by carrying out a 1-h incubation with the labelled anti-IgG on small squares with the immobilised IgG (specific binding) and on small squares with only activated carboxylic groups without immobilised IgG (nonspecific binding). In this second case, the COOH groups were treated with 0.2 M tris-HCl, pH 7.5, in order to block the activated surface for the covalent immobilisation. After the incubation, the small squares were rinsed with PBS and the fluorescence spectra were collected. These tests were performed on small squares treated with Eudragit L100 (0.01 mM), PLLA (0.01 mM) and 2 M NaOH (in 1:1

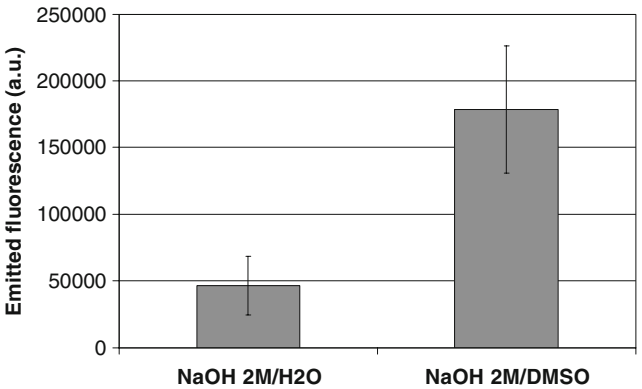

Fig. 7 Histogram of the emitted fluorescence of the small squares treated with 2 M NaOH in H_2O and with 2 M NaOH in a 1:1 mixture of water and DMSO, evaluated by considering the area of the collected spectra between 650 and 750 nm. The *error bars* give the standard deviations on three measurements performed on three different squares

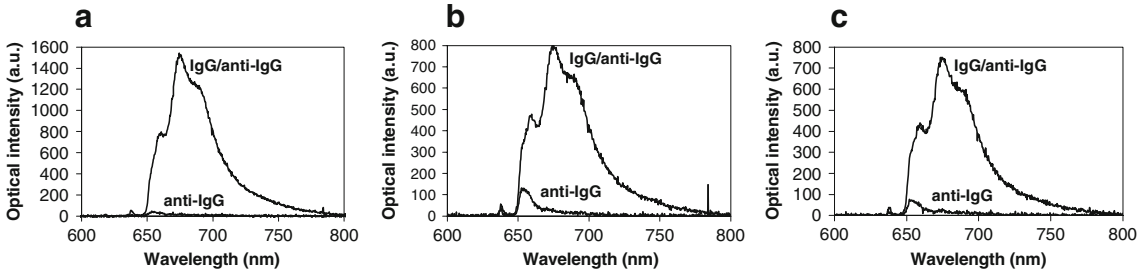

Fig. 8 Fluorescence emission spectra of the small PMMA squares treated with **a** 0.01 mM Eudragit L100, **b** 0.01 mM PLLA, **c** 2 M NaOH (in 1:1 H_2O/DMSO), with (*upper spectrum*) and without (*lower spectrum*) immobilised IgG, after 1-h incubation with the labelled anti-IgG. Measurements were carried out with the optical setup shown in Fig. 2. The small peak at 635 nm is the residual scattered light from the source properly filtered

water/DMSO) and the resulting fluorescence spectra are shown in Fig. 8a–c, respectively. In all cases, the nonspecific binding was negligible, with the best performance exhibited by the surface treated with Eudragit L100. Therefore, the treatment with tris-HCl was sufficiently efficient to prevent the nonspecific binding and this procedure was applied in all the further measurements described. In these experiments, the contribution coming from the source was filtered using the HP filter (cut-on at 650 nm) with the consequent almost total removal of the source peak.

Eudragit L100 (0.01 mM) was selected in order to identify the optimal concentration of IgG to be used for the formation of the sensing layer on the PMMA chip. Three different IgG concentrations (0.005, 0.05 and 0.5 mg mL^{-1}) were deposited on the chip. After 1-h incubation with 0.1 mg mL^{-1} of labelled anti-mouse-IgG, the chip was interrogated with the optical configuration shown in Fig. 3, without the cylindrical lens and the input BP filter at 635 nm. The obtained results are shown in Fig. 9.

The fluorescence signal is centred around 670 nm, whereas the peak centre around 655 nm is the contribution coming directly from the source due the scattering. Although the signal levels and the efficiency of the fluorescence collection are low, the results shown in Fig. 9 give the clear indication that 0.05 mg mL^{-1} is the optimal concentration of IgG to cover the PMMA surface. The reason for the lower signal level obtained with the PMMA chip compared with the small PMMA squares (shown in Fig. 8) is due to two main factors:

1. The different dimensions of the luminous spot useful for producing fluorescence: in the case of the small squares, almost the whole surface of the square (1 cm^2) carries the labelled anti-IgG, whereas in the case of the channel in the PMMA chip the surface is limited by the dimension of the flow channel. Since the lateral dimension of the flow channel is 0.5 mm, the illuminated surface useful for producing fluorescence is estimated to be ca. 0.05 cm^2.
2. The labelled anti-IgG concentration used in the experiments shown in Fig. 9 is 0.1 mg mL^{-1}, i.e. ten times smaller than the concentration used in the experiments in Fig. 4.

The optical efficiency of the system was improved by positioning a cylindrical lens on the top of the PMMA chip in correspondence with the sensing layer (Fig. 3b), which allows one to focus the LD beam on the immobilised sensing layer. A further improvement was obtained by replacing the Ocean Optics spectrometer with the Hamamatsu spectro-

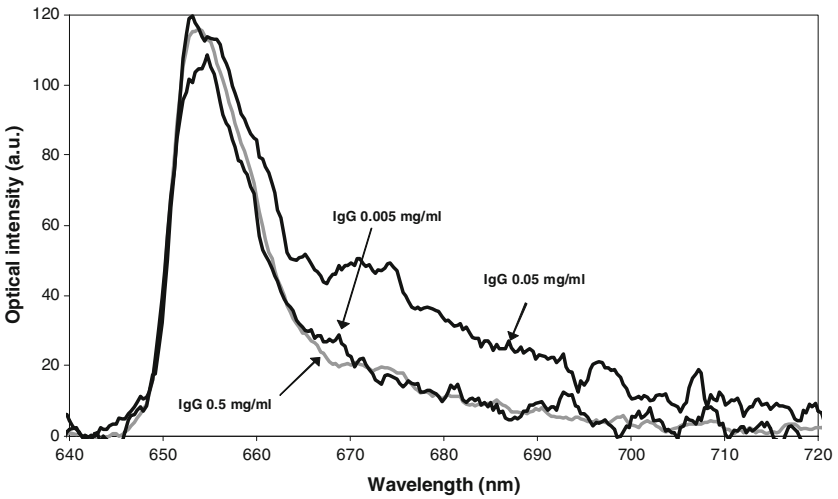

Fig. 9 Optical intensity detected with the PMMA chip in the case of three different mouse IgG concentration deposited on 0.01 mM Eudragit L100. The signal is recorded after 1-h incubation with 0.1 mg mL^{-1} of labelled anti-IgG

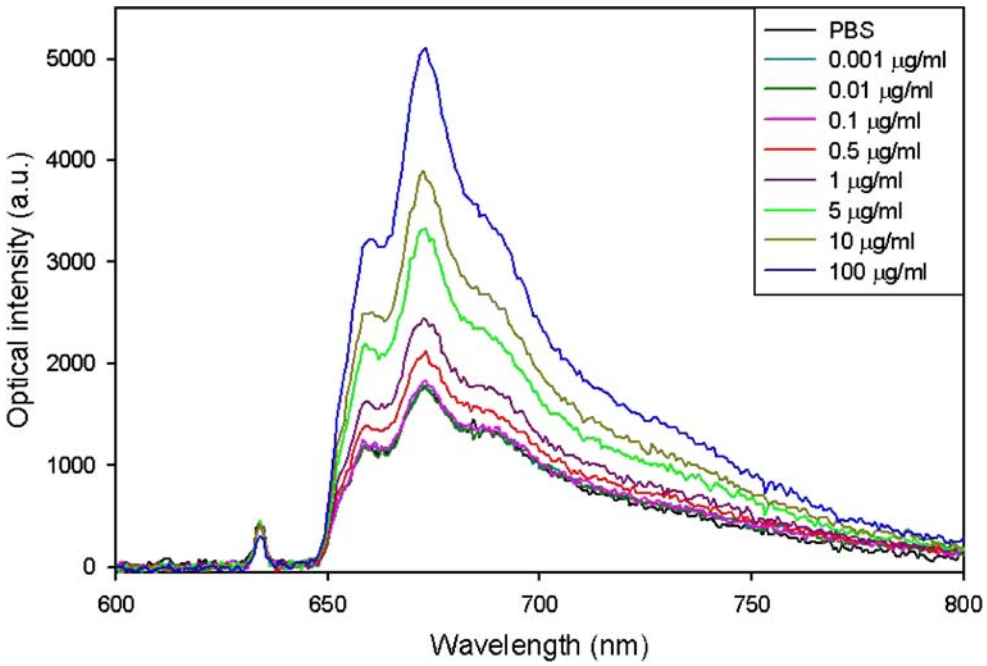

Fig. 10 Fluorescence emission spectra coming from the PMMA chip in the case of treatment with Eudragit L100, for different concentrations of labelled anti-IgG

meter. This produced an enhancement of about one order of magnitude in the signal to noise ratio (SNR). Also the contribution from the scattered light coming from the source, represented by the peak at 655 nm in Fig. 9, was noticeably reduced by placing the BP filter at 635 nm in front of the source.

On the basis of the results shown in Fig. 9, the IgG/anti-IgG assay was then performed by immobilising 0.05 mg mL^{-1} IgG on the PMMA chip, previously treated with either 0.01 mM Eudragit L100, 0.01 mM PLLA or 2 M NaOH in DMSO/H_2O.

The level of improvement in the optical efficiency can be appreciated from Fig. 10, which shows the fluorescence spectra in the case of treatment with Eudragit L100, for different concentrations of labelled anti-IgG (the spectra should be compared with those shown in Fig. 9). The measurements were carried out in flow mode according to the protocol described previously. It is also important to stress that in this case the incubation time was reduced to 15 min. This is a very important parameter in the design and development of clinical assays, especially those for point of care applications, where the reduction of the duration of the assay is an essential requirement. The spectra were recorded after the 5-min washing with PBS. Each spectrum is the average of ten spectra acquired with an integration time of 10 s. A fluorescence signal was also

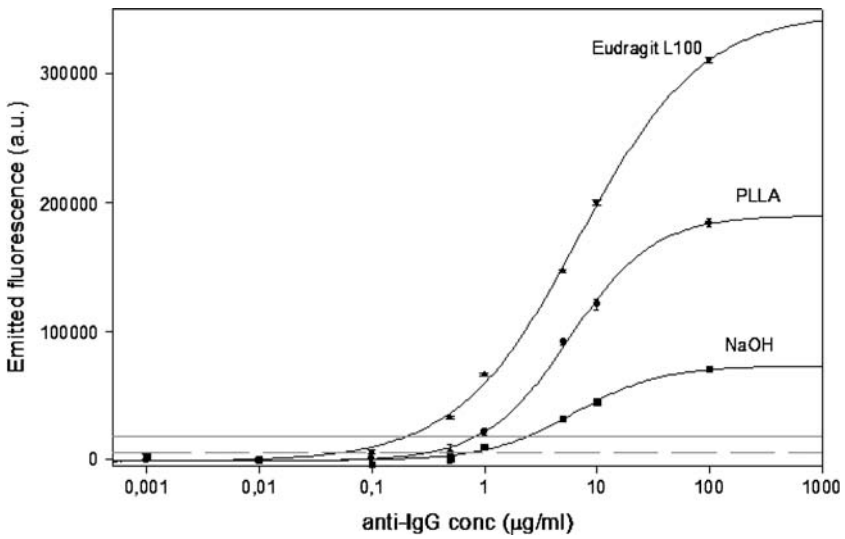

Fig. 11 Calibration curves of the IgG/anti-IgG assay for the three different treatments of the PMMA surface. The *horizontal lines* are drawn considering three times (*dashed line*) and ten times (*solid line*) the highest value of the standard deviation calculated on the different points for the curve related to Eudragit L100

observed in the case of PBS buffer alone, without any labelled molecules bound to the IgG layer. The spectrum in this case overlaps with the 0.001 μg mL^{-1} spectrum, shown in Fig. 10, and this spectrum represents the zero of this series of measurements. This effect is mainly due to the autofluorescence of PMMA which implied the presence of an intrinsic background in the detected signals. It is worthwhile mentioning that the PMMA, if produced by injection moulding, is characterised by low autofluorescence, when excited in the red region [18]. In our case the provider of PMMA was unable to give this information.

The fluorescence signal detected in the presence of PBS is not due only to autofluorescence of PMMA but there is a small contribution caused by the fluorescence coming from the bottom surface of the microchannel. During all the measurements we always used the same bottom part, changing only the upper part carrying the sensing layer. This caused a sort of aging of the bottom PMMA surface by the adhesion of molecules of labelled anti-IgG which were not removed. On the other hand the coupling efficiency of immobilised fluorophore on the bottom part was very low, since the emitted fluorescence crosses the cover without any possibility of being guided along the thickness of the chip. Consequently the signal coming from the bottom was a small constant background which can be added to the autofluorescence.

Figure 11 illustrates the calibration curves for the three different cases, i.e. PMMA treatment with NaOH, Eudragit L100 and PLLA; the fitting of the experimental points with a sigmoid curve is also shown. The contribution of the fluorescence background to the fluorescence signal was ignored, since the value obtained using pure PBS sample was zero. The integral between 650 and 750 nm of each spectra was evaluated and each point of the graph was obtained by calculating the average value on a total of ten recorded spectra and the standard deviation is also shown.

The best performance was obtained with Eudragit. The corresponding limits of detection and of quantification were evaluated: the horizontal lines shown in Fig. 11 were drawn considering three times (dashed line) and ten times (solid line) the highest value of the standard deviation calculated on the different points for the curve related to Eudragit. The intercept with the calibration curve gives the limit of detection, 0.05 μg mL^{-1}, and the limit of quantification 0.2 μg mL^{-1}, for the IgG/anti-IgG assay.

Conclusions

The described optical platform, based on the anisotropy of the fluorescence at the interface between two different means, was optimised for the implementation of bioassays. The system was characterised with the IgG/anti-IgG assay and the obtained results are satisfactory. The optical efficiency of the system can be further improved if the spectrum analyser is replaced by a photomultiplier or a powerful detector, without discriminating the detected wavelength. On the other hand the described system, equipped with the spectrum analyser, was essential in the identification of the better working wavelengths and in the discrimination of the optical signal coming from the chip (fluorescence and scattered light). It is also important to stress the particular configuration of the chip with multiple channels, which is potentially useful for multianalyte assay, with each single channel designed for the detection of different analytes.

Acknowledgments This research study was supported by the European Community within the framework of the five-year EU funded project under IST priority, CAREMAN (HealthCARE by Biosensor Measurements and Networking). The authors wish to thank Lorena Tedeschi of the Institute of Clinical Physiology of Pisa for her positive collaboration and fruitful suggestions.

References

1. Vo-Dinh T (2003) Biochips and microarrays: tools for the new medicine. In: Vo-Dinh T (ed) Biomedical photonics handbook. CRC, Boca Raton
2. Vo-Dinh T, Cullum B (2000) Fresenius J Anal Chem 366:540–551
3. Ligler FS, Taitt CAR (eds) (2002) Optical biosensors: present & future. Elsevier, Amsterdam
4. Homola J, Lu HB, Nenninger GG, Dostàlek J, Yee SS (2001) Sens Actuat B 76:403–410
5. Gauglitz G, Brecht A, Kraus G, Nahm W (1993) Sens Actuat B 11:21–27
6. Dieterle F, Belge G, Betsch C, Gauglitz G (2002) Anal Bioanal Chem 374:858–867
7. Ligler FS, Rowe-Taitt CA, Shriver-Lake LC, Sapsford KE, Shubin Y, Golden JP (2003) Anal Bioanal Chem 377:469–477
8. Barzen C, Brecht A, Gauglitz G (2002) Biosens Bioelectron 17:289–295
9. Epstein JR, Biran I, Walt DR (2002) Anal Chim Acta 469:3–36
10. Proll G, Tschmelak J, Gauglitz G (2005) Anal Bioanal Chem 381:61–63
11. Blum LJ, Marquette CA (2006) Chemiluminescence-based sensors. In: Baldini F, Homola J, Martellucci S, Chester A (eds) Optical chemical sensors. NATO Science Series, Springer, The Netherlands
12. Proll G, Steinle L, Proll F, Kumpf M, Moehrle B, Mehlmann M, Gauglitz G (2007) J Chromatogr A 1161:2–8
13. Moreno-Bondi MC, Taitt CR, Shriver-Lake LC, Ligler FS (2006) Biosens Bioelectron 21:1880–1886
14. Preininger C (2006) DNA and protein arrays. In: Baldini F, Homola J, Martellucci S, Chester A (eds) Optical chemical sensors. NATO Science Series, Springer, The Netherlands
15. Stuart H, Hall D (1998) Phys Rev Lett 80:5663–5666
16. Polerecky L, Hamrle J, MacCraith BD (2000) Appl Opt 39:3968–3977
17. Baldini F, Carloni A, Falciai R, Giannetti A, Mencaglia A, Porro G, Trono C (2007) Optical PMMA chip for multianalyte detection. In: Cutolo A, Culshaw B, Lòpez-Higuera JM (eds) Third European Workshop on Optical Fibre Sensors. Proceedings of SPIE 6619:661923-1-661923-4
18. Piruska A, Nikcevic I, Lee SH, Ahn C, Heineman WR, Limbacha PA, Seliskar CJ (2005) Lab on Chip 5:1348–1354